

Integrated Optical Polarization of Nearby Galaxies

Amy Jones

Lifan Wang

Kevin Krisciunas

Emily Freeland

*George P. & Cynthia W. Mitchell Institute for Fundamental Physics and Astronomy,
Department of Physics and Astronomy, Texas A&M University, College Station, TX
77843, USA*

ymamay@physics.tamu.edu

ABSTRACT

We performed an integrated optical polarization survey of 70 nearby galaxies to study the relationship between linear polarization and galaxy properties. To date this is the largest survey of its kind. The data were collected at McDonald Observatory using the Imaging Grism Polarimeter on the Otto Struve 2.1m telescope. Most of the galaxies did not have significant level of linear polarization, where the bulk is $< 1\%$. A fraction of the galaxies showed a loose correlation between the polarization and position angle of the galaxy, indicating that dust scattering is the main source of optical polarization. The unbarred spiral galaxies are consistent with the predicted relationship with inclination from scattering models of $\sim \sin^2 i$.

Subject headings: Magnetic Fields – Polarization – Scattering – Surveys – Galaxies: ISM

1. Introduction

Measuring optical polarization is a powerful method for probing the geometry and composition of dust in galaxies because the data contain directional and intensity information (Hall 1949; Hiltner 1949; Whittet 2003). Polarization studies have been done on a variety of objects, including stars in the Milky Way (MW) (Heiles 2000; van Smith 1956; Mathewson & Ford 1970), accretion disks around black holes (Antonucci 1984; Stockman et al.

1984; Wills et al. 1992; Brindle et al. 1990), and young stellar objects (Bastien & Menard 1990). Measuring optical polarization of galaxies is a key way to learn more about their dust and magnetic field properties.

Studies of stars in our galaxy indicate that optical polarization arises from directional absorption or scattering by aligned elongated dust grains in the interstellar medium (ISM) (Whittet 2003; Mathewson & Ford 1970; Axon & Ellis 1976) commonly known as the Davis-Greenstein effect (Davis & Greenstein 1951). These grains align themselves with their long axis perpendicular to the interstellar magnetic field (Wood 1997; Lazarian 2003). Light that is polarized parallel to the magnetic field, along the short axis of the dust grain, is more likely to pass through the ISM without being absorbed or scattered. Thus, the observer sees linear optically polarized light that is parallel to the galactic plane. The amount of light that is polarized is typically between 0% and 5%, with a few sightlines showing polarizations as high as 12%, depending on the amount and type of dust (Heiles 2000).

The other source of extragalactic optical polarization is by dust scattering (Brown & McLean 1977; Thompson et al. 1980; Simmons 1982). Light scattered off of particles will be polarized, as in the classic example of the light scattering off Earth’s atmosphere causing the sky to be polarized. The polarization of scattered light depends on the distribution of dust in the disk, and so the polarization angle can also be correlated with the galactic plane. In this case the polarization would be perpendicular to the plane of the galaxy. There have been several models of scattering in both optically thin and thick spiral galaxies and with Mie, Thomas, and Rayleigh scattering (Bianchi et al. 1996; Wood & Jones 1997; Simmons & Audit 2000). They predict that the polarization should be related to the position and inclination angles, and be on the order of a few percent.

Most studies of polarization in extragalactic sources have been done at radio wavelengths. Radio synchrotron emission is naturally polarized and directly traces ordered magnetic fields in galaxies (Beck 2005). From extragalactic radio polarization surveys, spiral galaxies have coherent galactic magnetic fields that lie along the galactic plane (Tosa & Fujimoto 1978; Beck 1983). Some barred spiral galaxies have additional magnetic field structures associated with the bar (Beck et al. 2002). Stil et al. (2009) conducted an integrated radio polarization survey of 43 galaxies and observed that the percent polarization depends on the inclination, and the polarization angle is related to the angle of the galactic plane.

There have been few optical polarization measurements of external galaxies, and individual galaxies in these studies typically show optical linear polarization at the $\lesssim 1\%$ level (Serkowski et al. 1975; Brindle et al. 1991; Sofue et al. 1986). The results of these studies are mainly consistent with optical polarization arising by the Davis-Greenstein effect and a few cases from scattering (Wood & Jones 1997; Simmons & Audit 2000).

Most of the previous optical polarization studies of galaxies were spatially resolved (Sofue et al. 1986; Scarrott et al. 1990; Draper et al. 1995), with a few exceptions where only certain types of galaxies were targeted (Brindle et al. 1990, 1991). Scarrott et al. (1990) and Sofue et al. (1986) produced optical polarization maps of 7 and 13 galaxies, respectively, and found that only those with ordered dust lanes, such as Sa type galaxies (e.g. M104) had a significant amount of polarization, $\sim 4-5\%$ along the galactic plane. Integrated polarization should be less than what is measured from the polarization maps. Cancellations arise from integrating the polarization vectors over the entire galaxy. These vectors are not well ordered, especially at larger radii, and will partially cancel each other. Serkowski et al. (1975) studied integrated optical polarization of 14 galaxies. Most of their galaxies were ellipticals (9 of the 14) and were taken without a filter. The highest value was from NGC 7041 with a linear polarization of $0.68 \pm 0.12\%$, and the average for the 14 galaxies was 0.38% . Brindle et al. (1991) observed starbursting and interacting galaxies in optical/infrared polarization and found that most of them were $< 1\%$ polarized.

Our integrated optical polarization survey of nearby galaxies is currently the largest survey of this type, with data for 70 galaxies presented in this paper. If dust alignment or scattering is the main source of optical polarization, then we would expect the linear polarization to correlate with the galaxy’s position angle, morphological type, and inclination angle (Simmons & Audit 2000; Bianchi et al. 1996).

2. Data Collection and Analysis

The data were collected at McDonald Observatory with the 2.1m Otto Struve telescope using the Imaging Grism Polarimeter (IGP) (Trammell 1994). Targets were selected from the Uppsala General Catalogue (UGC). They needed to fit within the $\sim 1'$ diameter field of view (FOV) and to be brighter than 16th magnitude (Nilson 1973). Selected galaxies were located $> 20^\circ$ off the galactic plane (with one accidental exception) and had low levels of dust extinction $E(B - V) \lesssim 0.1$, to minimize Milky Way foreground polarization (Burstein & Heiles 1982; Schlegel et al. 1998). There was a preference for galaxies with a star $\sim 0.5'$ away, close enough to be within the FOV and far enough to not intermingle with the galaxy. The information used for target selection came from NASA’s Extragalactic Database (NED) and the Uppsala General Catalogue (UGC). A range of morphological types and inclination angles was chosen. Due to the size and brightness constraints, there was a selection bias towards S0 and Sa type galaxies (de Vaucouleurs et al. 1991). All of the target galaxies are thought to be isolated with the exception of a few known to be galaxy pairs.

We conducted imaging polarimetry in the B-band over two observing runs, November 2008 and December 2009. For each galaxy, exposures were taken with the optical axis oriented to 0° , 45° , 22.5° , and 67.5° with respect to North, calibrated with the polarized standard stars’ published polarization angles. Exposure times ranged from 100 s to 200 s depending on the surface brightness of the galaxy, and each galaxy was imaged two or three times per orientation.

Standard stars from Schmidt et al. (1992) and Turnshek et al. (1990) were observed throughout the observing runs. During the first observing run only three unpolarized standard stars and two polarized stars could be used for data analysis. (HD 251204 is a known variable according to Amirkhanyan (2006); Weitenbeck (1999); Ogle et al. (1999)) For the second observing run, seven unpolarized and eight polarized standard stars were observed, two each per night with the exception of 19 December 2009 where we had observations of only one unpolarized standard.

All the images were bias corrected using IRAF, and the rest of the analysis, including flat fielding, was done with IDL. The signal-to-noise ratios of the pixel with the highest counts in the reduced images were ~ 100 . In the IGP, there is a polarizing calcite beam splitter, so each exposure produced two images of an object in orthogonal polarization states, hereafter called top and bottom. After imaging at each of four different orientation angles an object had eight associated images. Images of the same galaxy with the same waveplate position angle were stacked by aligning the centers of the object.

The flux from the objects was multiplied by a 2-D Gaussian weight function G that allowed us to more heavily weight the data from the bright center of the galaxies compared to the faint edges where the signal to noise was low (Rhodes et al. 2000).

$$G = \frac{1}{2\pi\sigma_G^2} \exp \left[-\frac{1}{2\sigma_G^2} \left((x - x_0)^2 + (y - y_0)^2 \right) \right]. \quad (1)$$

The values x_0 and y_0 correspond to the center of the galaxy. The standard deviation σ_G in Equation 1 and the radius of the circle that was summed within were chosen to minimize the contribution of read-out noise and maximize the signal to noise ratio. The radius ranged between $3''$ and $23''$ and is listed, along with σ_G , in Table 3. The normalized Stokes q and u vectors were calculated by following the convention of Trammell (1994). The main equations are given below, where I is the total intensity and $f_{angle,t/b}$ is the integrated, weighted flux for either the top or bottom image with the optical axis at the given angle.

$$q = \frac{Q}{I} = \frac{1}{2} \left(\frac{f_{0^\circ,t} - wf_{45^\circ,t}}{f_{0^\circ,t} + f_{45^\circ,t}} - \frac{f_{0^\circ,b} - wf_{45^\circ,b}}{f_{0^\circ,b} + f_{45^\circ,b}} \right), \quad (2)$$

$$u = \frac{U}{I} = \frac{1}{2} \left(\frac{f_{22.5^\circ,t} - wf_{67.5^\circ,t}}{f_{22.5^\circ,t} + f_{67.5^\circ,t}} - \frac{f_{22.5^\circ,b} - wf_{67.5^\circ,b}}{f_{22.5^\circ,b} + f_{67.5^\circ,b}} \right). \quad (3)$$

The w is a weighting factor to correct for changes in the flux due to differences in atmospheric transparency, see Trammell (1994) for more details.

With the normalized Stokes q and u vectors it is then straightforward to calculate the linear percent of polarization and the polarization angle (direction of the polarization E-vector):

$$P^2 = q^2 + u^2, \quad (4)$$

$$\theta_{pol} = \frac{1}{2} \arctan \frac{u}{q}. \quad (5)$$

The percent polarization was corrected for a positive bias following the procedures outlined by Wang et al. (1997). They used a simple method for optimization of the marginal distribution (Simmons & Stewart 1985) to find the true values P^{true} and θ_{pol}^{true} by,

$$P^{true} = P - \sigma^2/P H(P - \sigma), \quad \theta_{pol}^{true} = \theta_{pol}. \quad (6)$$

Here H is the Heaviside function and σ is the Poisson error based on photon statistics for the integrated polarization P , which includes all sources of error and is listed in Table 3.

The position angle of a galaxy on the sky, defined here as the projected angle to the major axis of the brightest galactic feature from North, was determined using the second moment of the flux $f(x, y)$ after applying the Gaussian weight function G (Equation 1). For face-on galaxies, the position angle gives the general direction of any bright internal structure, like bars and spiral arms, which from radio polarimetry traces the magnetic field (Beck 2005). For edge-on galaxies, it traces the major axis of the the disk. Both the polarization and position angle are calculated after applying the Gaussian weight function G to allow for a direct comparison. The position angle is given by the following equation.

$$\theta_{pa} = \frac{1}{2} \arctan \frac{2I_{xy}}{I_{xx} - I_{yy}}, \quad (7)$$

where,

$$\begin{aligned} I_{xx} &= \int dx dy (x - x_0)^2 G f(x, y), \\ I_{yy} &= \int dx dy (y - y_0)^2 G f(x, y), \\ I_{xy} &= \int dx dy (x - x_0) (y - y_0) G f(x, y). \end{aligned} \quad (8)$$

The position angles calculated are all consistent with published values, with a few exceptions (i.e. Nilson (1973)). The position angles of UGC 3709, 4227, 4556, and 5339NED01

differed from the published ones because they were calculated with the Gaussian weight function which traced the bugle instead of the disk. For UGC 545, 4851, and 5097, the published values were used instead of the calculated position angles. For these galaxies, with the Gaussian weight function, it was difficult to calculate decent position angles due to either stray star light from a foreground star or the inner regions were too clumpy. For UGC 758, 1150, 1359, 2143, 3258, 3414, 3930, 11734, and 12608, position angles are published only in the infrared and deviate from our calculated angles by more than 10° .

For the polarization percent and angle, and position angle, Poisson errors were assumed and propagated through the calculations. According to Trammell (1994), the instrumental polarization errors for the IGP are $\leq 0.1\%$ which is consistent with the linear polarization values that we measure in our polarized standard stars. Table 1 lists the unpolarized standard star observations and Table 2 lists the polarized standard star observations with the measured and published amounts of linear polarization for each star in the Johnson B-filter (Schmidt et al. 1992; Turnshek et al. 1990).

UGC 1236 and 1260, were observed during both observing runs to check for consistency. Their measured polarization percentages and angles, as well as the calculated position angle on the sky were in agreement for the two observing runs.

Additionally, the inclination angle i was calculated using the values of the semi-major a and semi-minor b axis given in the NASA Extragalactic Database (NED) (Nilson 1973) by the following equation,

$$\cos^2 i = \frac{(b/a)^2 - q_0^2}{1 - q_0^2}. \quad (9)$$

Here, q_0 is the intrinsic axial ratio and for a typical spiral galaxy is 0.2 (Tully 1988).

There is a large amount of uncertainty in the inclination angles and the axes here are measured in unpolarized light. They are sufficient for the purposes of this paper, since we are only concerned with the overall relationship between the polarization and inclination angle.

An approximation of the MW foreground polarization is the color excess $E(B - V)$ (Burstein & Heiles 1982). Note, there is about a 10% error in $E(B - V)$. This is a measure of the extinction from the MW, to the target, along the line of sight. Serkowski et al. (1975) empirically found that the maximum optical polarization along a sightline is $\lesssim 9 \times E(B - V)$. To ensure that the polarization measured was not solely from the MW, all galaxies used in the data analysis have levels of polarization that are $\geq 9 \times E(B - V)$ (Figure 1).

UGC 3414 is a good example showing that the extinction cut is valid. UGC 3414

and the two stars in the FOV all had similar polarization levels and angles. Its maximum MW polarization based on the color excess $E(B - V)$ was also comparable to the measured polarization, within 1σ . In this case the MW foreground contamination is the dominant source of polarization and the galaxy was removed from the analysis based on its extinction.

Table 3 presents the radius r and σ_G used in the Gaussian weight function G , percentage of linear polarization, polarization angle, position angle of the galaxy on the sky, as well as morphological type, MW extinction $E(B - V)$ and inclination angle from NED for the galaxies in this study (de Vaucouleurs et al. 1991; Burstein & Heiles 1982; Nilson 1973). Galaxies that were not used in the data analysis are presented below the line in Table 3. They either had polarizations that were less than twice the errors (similar to the cuts made by Brindle et al. (1991)), or appear to be highly contaminated by MW polarization based on MW extinction $E(B - V)$. The distributions of the polarization values before and after the cuts are shown in Figure 2. The majority of galaxies with $\leq 0.6\%$ are not used in the analysis. Most of the galaxies used in the analysis are around 1% linearly polarized, with a mean average polarization of 0.94%. This is consistent with previous optical polarization studies (Serkowski et al. 1975; Sofue et al. 1986; Scarrott et al. 1990; Brindle et al. 1991; Draper et al. 1995).

3. Discussion

The low levels of integrated linear polarization reported in this and previous studies may be caused by MW foreground contamination, nonuniform dust distributions inside the host galaxies, and a reduction in the integrated signal from cancellations. First, MW polarization is of the same order as the polarization from the bulk of the target galaxies. Even though we have removed galaxies dominated by MW foreground polarization, the MW could still contaminate and depolarize the signal of the target galaxies. Second, for directional absorption or scattering to occur, the dust grains need to be distributed somewhat uniformly about the galactic plane. For directional absorption, a fraction of the dust grains also need to align themselves with the magnetic field (Whittet 2003). In scattering, theoretical papers assume that the dust grains are uniform and predict polarizations around 1 to 2% (Bianchi et al. 1996; Wood & Jones 1997; Simmons & Audit 2000). Lastly, the amount of polarization could also be diminished due to cancellations from integrating over the whole galaxy arising from non-uniformity of the galactic magnetic field. All of these issues probably contribute to the overall low levels of polarization.

Other optical polarization studies discuss having difficulty with the MW foreground. In a study of optical/infrared polarization of Seyfert galaxies, Brindle et al. (1990) claim

that any linear polarizations less than 0.5% can arise from the MW. From their simulation for their sample, the median degree of MW polarization was 0.6%. One of the advantages of having a large sample is the ability to avoid galaxies with a high probability of being contaminated with MW polarization. In doing so, our initial sample size was cut in half. Since our average polarization after the cuts is 0.9%, we are confident that our sample is above the noise of the MW foreground, which is $\sim 0.5\%$ based on the average $E(B - V)$.

We find a loose correlation between the position angle of the galaxy and its integrated polarization angle, indicating that the polarization arises from scattering off of dust grains that are distributed along the galactic plane. We examine this correlation by looking at the distribution of the difference of these two angles folded about 90° , shown in Figure 3. In the distribution we expect peaks around 0° for dust alignment or 90° for scattering of the positive difference between the polarization and position angles. There is a peak around 90° , indicating that dust scattering is the dominant process of optical polarization. From Monte Carlo simulations, there is less than a 10% probability that this peak is random. This finding is contradictory to what is seen in the MW optical polarization and some of the optical polarization maps of other galaxies, which are caused by dust alignment (Whittet 2003; Scarrott et al. 1990). The reason for this discrepancy is unclear.

Galaxies with polarization levels greater than 1.5% are less than 15° away from having their polarization being perpendicular to their position angles. The galaxies with the highest level of polarization are consistent with scattering being the source of polarization. The exception is UGC 545, which has the angles being parallel. UGC 545 is a known Seyfert I galaxy according to NED (de Vaucouleurs et al. 1991). The polarization from this galaxy is most likely due to its active galactic nucleus (AGN) and not from the galaxy. UGC 545 has a level of polarization of 2.3%. Seyfert I galaxies tend to have polarizations $\sim 2.9\%$ compared to the average of this sample of 1.0%, indicating that UGC 545’s polarization comes from its AGN (Antonucci 1984).

There is a lack of evidence from this study showing that the level of polarization depends on the morphological type. Naively one would expect the polarization in spirals to be higher due to the coherent magnetic fields and higher amount of structure compared to irregulars and ellipticals (Beck 2005; Chyży et al. 2003). Above 1% polarization spiral galaxies are the only morphological type present, as shown in Figure 4, however the majority of the sample is composed of spirals. The mean average linear polarization for spiral galaxies is 1.0%, whereas the mean average of the four irregulars is 0.81% and the one elliptical galaxy is 1.0%. A larger sample is needed to conclude whether there is a correlation between the percent of polarization and the morphological type of galaxies.

The polarization level of unbarred spiral galaxies generally increases with inclination

angle and barred spirals stay roughly constant, at $\lesssim 1.0\%$, as shown in Figure 5. The polarizations of unbarred spiral galaxies are predicted to vary as $\sin^2 i$ and the galaxies in this sample loosely follow this relationship (Bianchi et al. 1996; Simmons & Audit 2000). A similar trend was found in an integrated radio polarization survey (Stil et al. 2009). Galactic magnetic fields are toroidal (Han & Wielebinski 2002), so less inclined galaxies should have more of their polarization cancel out from the integration. However, bars in spiral galaxies have been shown to have additional magnetic fields associated with them (Beck 2005), so a face-on barred spiral could have a higher polarization level due to the contribution from the bar.

4. Summary

We have presented the results of an integrated optical polarization survey of 70 nearby galaxies in order to study the relationship between linear polarization and galactic properties.

- The average level of linear optical polarization of galaxies in this survey that were used in the analysis is 0.9% (Figure 2). Seven of the galaxies that were used for the analysis had polarization greater than 1%. This is consistent with previous optical polarization studies of galaxies.

- There is a loose correlation between the galactic polarization angle and the position angle (Figure 3). There is a peak in the distribution of the positive difference between the polarization and position angle around 90 degrees indicating that the polarization is perpendicular to the galactic plane. This suggests that the galactic optical polarization arises from scattering. From Monte Carlo simulations, there is less than a 10% chance that this peak is random.

- There is no evidence that the level of polarization depends on morphological type (Figure 4).

- For unbarred spiral galaxies the polarization tends to increase with inclination angle loosely following the predicted $\sin^2 i$ relationship from scattering (Bianchi et al. 1996; Simmons & Audit 2000). Barred spirals have a fairly flat distribution (Figure 5). This is consistent with the Stil et al. (2009) study using radio polarization.

We thank McDonald Observatory for the access to the Otto Struve 2.1m telescope. We would also like to thank the anonymous referee for the detailed suggestions. This research has made use of the NASA/IPAC extragalactic database (NED), which is operated by the Jet Propulsion Laboratory, Caltech, under contract with the National Aeronautics and Space

Administration. This work was supported by Texas A&M University funds made available to Lifan Wang.

REFERENCES

- Amirkhanyan, V. R. 2006, *Astronomy Reports*, 50, 273
- Antonucci, R. R. J. 1984, *ApJ*, 278, 499
- Axon, D. J. & Ellis, R. S. 1976, *MNRAS*, 177, 499
- Bastien, P. & Menard, F. 1990, *ApJ*, 364, 232
- Beck, R. 1983, in *IAU Symposium*, Vol. 100, *Internal Kinematics and Dynamics of Galaxies*, ed. E. Athanassoula, 159–+
- Beck, R. 2005, in *Lecture Notes in Physics*, Berlin Springer Verlag, Vol. 664, *Cosmic Magnetic Fields*, ed. R. Wielebinski & R. Beck, 41–+
- Beck, R., Shoutenkov, V., Ehle, M., Harnett, J. I., Haynes, R. F., Shukurov, A., Sokoloff, D. D., & Thierbach, M. 2002, *A&A*, 391, 83
- Bianchi, S., Ferrara, A., & Giovanardi, C. 1996, *ApJ*, 465, 127
- Brindle, C., Hough, J. H., Bailey, J. A., Axon, D. J., & Sparks, W. B. 1991, *MNRAS*, 252, 288
- Brindle, C., Hough, J. H., Bailey, J. A., Axon, D. J., Ward, M. J., Sparks, W. B., & McLean, I. S. 1990, *MNRAS*, 244, 577
- Brown, J. C. & McLean, I. S. 1977, *A&A*, 57, 141
- Burstein, D. & Heiles, C. 1982, *AJ*, 87, 1165
- Chyży, K. T., Knapik, J., Bomans, D. J., Klein, U., Beck, R., Soida, M., & Urbanik, M. 2003, *A&A*, 405, 513
- Davis, Jr., L. & Greenstein, J. L. 1951, *ApJ*, 114, 206
- de Vaucouleurs, G., de Vaucouleurs, A., Corwin, Jr., H. G., Buta, R. J., Paturel, G., & Fouque, P. 1991, *Third Reference Catalogue of Bright Galaxies*, ed. Roman, N. G., de Vaucouleurs, G., de Vaucouleurs, A., Corwin, H. G., Jr., Buta, R. J., Paturel, G., & Fouqué, P.

- Draper, P. W., Done, C., Scarrott, S. M., & Stockdale, D. P. 1995, *MNRAS*, 277, 1430
- Hall, J. S. 1949, *Science*, 109, 166
- Han, J.-L. & Wielebinski, R. 2002, *cjaa*, 2, 293
- Heiles, C. 2000, *AJ*, 119, 923
- Hiltner, W. A. 1949, *Science*, 109, 165
- Lazarian, A. 2003, *J. Quant. Spec. Radiat. Transf.*, 79, 881
- Mathewson, D. S. & Ford, V. L. 1970, *MmRAS*, 74, 139
- Nilson, P. 1973, *Nova Acta Regiae Soc. Sci. Upsaliensis Ser. V*, 0
- Ogle, P. M., Cohen, M. H., Miller, J. S., Tran, H. D., Goodrich, R. W., & Martel, A. R. 1999, *ApJS*, 125, 1
- Rhodes, J., Refregier, A., & Groth, E. J. 2000, *ApJ*, 536, 79
- Scarrott, S. M., Rolph, C. D., & Semple, D. P. 1990, in *IAU Symposium, Vol. 140, Galactic and Intergalactic Magnetic Fields*, ed. R. Beck, R. Wielebinski, & P. P. Kronberg, 245–251
- Schlegel, D. J., Finkbeiner, D. P., & Davis, M. 1998, *ApJ*, 500, 525
- Schmidt, G. D., Elston, R., & Lupie, O. L. 1992, *AJ*, 104, 1563
- Serkowski, K., Mathewson, D. S., & Ford, V. L. 1975, *ApJ*, 196, 261
- Simmons, J. F. L. 1982, *MNRAS*, 200, 91
- Simmons, J. F. L. & Audit, E. 2000, *MNRAS*, 319, 497
- Simmons, J. F. L. & Stewart, B. G. 1985, *A&A*, 142, 100
- Sofue, Y., Fujimoto, M., & Wielebinski, R. 1986, *ARA&A*, 24, 459
- Stil, J. M., Krause, M., Beck, R., & Taylor, A. R. 2009, *ApJ*, 693, 1392
- Stockman, H. S., Moore, R. L., & Angel, J. R. P. 1984, *ApJ*, 279, 485
- Thompson, I., Stockman, H. S., Angel, J. R. P., & Beaver, E. A. 1980, *MNRAS*, 192, 53
- Tosa, M. & Fujimoto, M. 1978, *PASJ*, 30, 315

- Trammell, S. R. 1994, PhD thesis, THE UNIVERSITY OF TEXAS AT AUSTIN.
- Tully, R. B. 1988, Nearby galaxies catalog, ed. Tully, R. B.
- Turnshek, D. A., Bohlin, R. C., Williamson, II, R. L., Lupie, O. L., Koornneef, J., & Morgan, D. H. 1990, AJ, 99, 1243
- van Smith, E. P. 1956, ApJ, 124, 43
- Wang, L., Wheeler, J. C., & Hoefflich, P. 1997, ApJ, 476, L27+
- Weitenbeck, A. J. 1999, actaa, 49, 59
- Whittet, D. C. B., ed. 2003, Dust in the galactic environment
- Wills, B. J., Wills, D., Breger, M., Antonucci, R. R. J., & Barvainis, R. 1992, ApJ, 398, 454
- Wood, K. 1997, ApJ, 477, L25+
- Wood, K. & Jones, T. J. 1997, AJ, 114, 1405

Table 1. Unpolarized Standard Stars

Name	Night Observed	Measured Polarization(%)	Published Polarization (%)
HD 94851	11-28-08	0.080 ± 0.08	0.06 ± 0.02
HD 94851	11-29-08	0.14 ± 0.08	0.06 ± 0.02
BD +28°4211	11-30-08	0.18 ± 0.05	0.063 ± 0.023
HD12021 ^a	12-17-09	0.31 ± 0.03	0.112 ± 0.025
GD319	12-17-09	0.19 ± 0.1	0.045 ± 0.047
HD12021 ^a	12-18-09	0.28 ± 0.05	0.112 ± 0.025
HD14069	12-18-09	0.27 ± 0.1	0.111 ± 0.036
HD94851	12-19-09	0.0039 ± 0.05	0.06 ± 0.02
HD14069	12-20-09	0.31 ± 0.05	0.111 ± 0.036
GD319	12-20-09	0.13 ± 0.15	0.045 ± 0.047

^aHD 12021 is consistently higher than the published value and is likely no longer an acceptable unpolarized standard star.

Note. — All published values are from Schmidt et al. (1992), except for HD 94851 which is from Turnshek et al. (1990).

Table 2. Polarized Standard Stars

Name	Night Observed	Measured Polarization(%)	Published Polarization (%)
HD 245310	11-29-08	4.5 ± 0.05	4.550 ± 0.064
HD 251204 ^a	11-29-08	4.8 ± 0.08	-
BD +38°4058/Hilt 960	11-30-08	5.6 ± 0.1	5.648 ± 0.022
BD +59° 389	12-17-09	6.3 ± 0.07	6.345 ± 0.035
HD245310	12-17-09	4.6 ± 0.09	4.550 ± 0.064
BD +64°106	12-18-09	5.7 ± 0.07	5.506 ± 0.090
HD245310	12-18-09	4.6 ± 0.1	4.550 ± 0.064
BD+64°106	12-19-09	5.6 ± 0.07	5.506 ± 0.090
HD245310	12-19-09	4.5 ± 0.09	4.550 ± 0.064
BD +64°106	12-20-09	5.6 ± 0.07	5.506 ± 0.090
HD245310	12-20-09	4.5 ± 0.08	4.550 ± 0.064

^aHD 251204 is a variable according to Amirkhanyan (2006); Weitenbeck (1999); Ogle et al. (1999) and is not an acceptable polarized standard star.

Note. — All published values, except HD 251204, are from Schmidt et al. (1992).

Table 3. Galaxies

UGC	r (")	σ_G (")	Linear Polarization(%)	Polarization Angle ($^\circ$)	Position Angle ($^\circ$)	Morphological Type	$E(B - V)$	Inclination Angle ($^\circ$)
6	8.7	1.9	1.0 ± 0.2	122 ± 4	91 ± 6	pec	0.047	...
50	6.8	3.1	0.9 ± 0.2	100 ± 4	11 ± 1	Sab	0.035	74
108	11.2	5.0	0.7 ± 0.1	122 ± 5	58 ± 1	SBb	0.041	58
240	14.3	5.6	0.8 ± 0.1	13 ± 4	72 ± 1	SAB(rs)b	0.023	62
285	7.4	4.3	0.4 ± 0.1	138 ± 9	108 ± 1	Sa	0.041	77
425	11.8	5.0	2.9 ± 0.1	135 ± 1	41 ± 2	SB	0.039	34
529	9.3	3.1	0.9 ± 0.2	121 ± 6	95 ± 1	S0/a	0.061	84
540	19.8	5.6	0.5 ± 0.1	107 ± 5	130 ± 1	Sb	0.053	53
545	5.6	1.2	2.3 ± 0.1	144 ± 3	150 ± 10^b	Sa	0.065	0
555	8.7	2.5	0.9 ± 0.1	118 ± 5	28 ± 4	S0/a	0.056	84
697	16.7	5.0	0.6 ± 0.1	100 ± 6	79 ± 1	SB	0.049	58
796	12.4	2.5	0.6 ± 0.1	11 ± 4	41 ± 7	S	0.058	30
1086	10.5	3.7	0.5 ± 0.1	138 ± 8	48 ± 1	S	0.043	69
1220	13.6	5.6	1.2 ± 0.1	119 ± 3	4 ± 1	Spec	0.054	53
1236 ^a	9.9	2.5	0.8 ± 0.2	102 ± 6	81 ± 2	S	0.043	46
1251	9.9	2.5	0.5 ± 0.2	92 ± 9	40 ± 1	S/Irr	0.055	58
1359	13.6	3.7	0.8 ± 0.1	109 ± 5	61 ± 3	SB/Sb	0.054	30
1467	12.4	5.6	0.7 ± 0.1	142 ± 3	85 ± 1	S	0.050	53
2143	11.2	5.0	0.6 ± 0.1	126 ± 4	45 ± 1	Irr	0.051	...
3258	3.1	1.9	0.9 ± 0.1	131 ± 5	98 ± 4	SB(r)ab pec	0.068	30
3885	17.4	7.4	0.6 ± 0.1	167 ± 4	84 ± 1	S	0.049	26
3930	13.0	5.0	0.7 ± 0.1	159 ± 3	119 ± 1	Im	0.049	...
4028	18.6	8.1	0.4 ± 0.1	108 ± 7	20 ± 1	SAB(s)c	0.028	29
4079	11.8	2.5	1.2 ± 0.1	13 ± 3	9 ± 2	Spec	0.040	62
4229	5.6	1.2	0.6 ± 0.2	170 ± 7	146 ± 40	S0	0.051	18
4249	8.7	4.3	2.7 ± 0.4	158 ± 3	55 ± 2	S	0.051	80
4438	15.5	6.8	0.5 ± 0.1	152 ± 4	13 ± 1	S(r) pec	0.047	30
4709	11.2	5.0	0.4 ± 0.1	171 ± 6	28 ± 1	S	0.024	41
4730	7.4	1.9	1.6 ± 0.1	7 ± 2	98 ± 2	S	0.043	74
4737	6.8	1.9	1.4 ± 0.1	50 ± 3	168 ± 20	S0	0.052	55
4813	7.4	2.5	0.9 ± 0.1	78 ± 4	161 ± 2	S	0.018	35
5097	11.2	3.7	0.5 ± 0.1	150 ± 4	55 ± 1^b	Sb	0.039	56
5132	11.2	5.0	0.8 ± 0.2	121 ± 7	29 ± 1	S	0.037	71
5200	8.1	1.9	1.0 ± 0.1	43 ± 4	144 ± 7	S0	0.025	30
5339 NED02	5.6	1.9	0.9 ± 0.2	11 ± 7	104 ± 10	Gpair	0.035	...
11734	21.7	8.7	1.0 ± 0.1	83 ± 4	46 ± 2	SBb	0.094	26
12329	9.9	3.1	1.0 ± 0.1	123 ± 4	25 ± 1	E3pec	0.085	...
12608	16.7	5.6	1.0 ± 0.1	61 ± 3	102 ± 2	SA(r)bc	0.059	25
NGC 7629	6.2	1.9	0.9 ± 0.1	120 ± 4	2 ± 3	SBO	0.044	38
644	9.3	4.3	0.6 ± 0.3	144 ± 10	69 ± 1	Gpair	0.043	...
644 NOTES01	6.2	3.1	0.6 ± 0.3	105 ± 10	18 ± 1	Gpair	0.043	...
645	7.4	2.5	0.3 ± 0.1	115 ± 10	41 ± 20	SB pec	0.045	62
758	18.0	6.8	0.4 ± 0.1	115 ± 4	83 ± 1	S	0.053	0
912	9.9	1.9	0.5 ± 0.1	110 ± 6	115 ± 1	...	0.060	...
1135	11.8	3.1	0.2 ± 0.2	93 ± 20	34 ± 6	S	0.042	53

Table 3—Continued

UGC	r (")	σ_G (")	Linear Polarization(%)	Polarization Angle ($^\circ$)	Position Angle ($^\circ$)	Morphological Type	$E(B - V)$	Inclination Angle ($^\circ$)
1150	19.2	6.2	0.5 ± 0.1	106 ± 4	111 ± 4	pec	0.067	...
1260 ^a	14.9	4.3	0.5 ± 0.1	108 ± 6	45 ± 1	(R')SB(s)a	0.093	42
1757	9.9	2.5	0.1 ± 0.1	161 ± 30	78 ± 1	S	0.057	81
2103	13.0	3.7	1.3 ± 0.1	150 ± 2	9 ± 1	S LIRG	0.149	40
2608	15.5	3.7	0.5 ± 0.1	144 ± 4	81 ± 1	(R')SB(s)b	0.160	28
3414	11.8	3.7	1.1 ± 0.1	170 ± 3	176 ± 1	S	0.129	0
3709	22.9	10.5	0.6 ± 0.1	172 ± 3	57 ± 1	S pec	0.072	22
3816	9.3	2.5	0.5 ± 0.1	178 ± 4	109 ± 4	S0	0.060	44
3969	11.2	4.3	0.1 ± 0.2	144 ± 50	135 ± 1	Scd	0.051	90
4041	15.5	3.7	0.3 ± 0.2	163 ± 20	127 ± 1	E	0.026	...
4111	18.0	6.2	0.2 ± 0.1	84 ± 8	173 ± 1	Sbcpec	0.046	44
4227	16.1	5.0	0.2 ± 0.1	149 ± 10	120 ± 3	SAB(rs)b	0.054	24
4287	16.7	3.1	0.3 ± 0.1	87 ± 6	174 ± 2	(R)SB(r)ab	0.041	28
4327	21.1	4.3	0.1 ± 0.1	130 ± 10	62 ± 1	(R')SB(s)a	0.026	44
4556	11.8	5.0	0.1 ± 0.2	177 ± 90	46 ± 1	Irr	0.029	...
4564	8.1	3.1	0.3 ± 0.2	0 ± 10	33 ± 1	Sc(f)	0.035	77
4580	13.0	5.0	0.1 ± 0.1	172 ± 30	11 ± 1	Sbc	0.034	62
4642	13.6	5.0	0.4 ± 0.2	174 ± 9	35 ± 1	S	0.027	32
4687	9.9	1.9	0.1 ± 0.1	113 ± 20	110 ± 10	pec	0.094	...
4741	13.0	5.0	0.5 ± 0.1	130 ± 3	67 ± 1	S	0.065	53
4823	11.2	4.3	0.2 ± 0.2	92 ± 20	173 ± 1	Sab	0.043	38
4851	7.4	2.5	0.1 ± 0.1	96 ± 20	150 ± 3^b	S0-	0.015	56
5022	9.3	2.5	0.1 ± 0.1	150 ± 40	177 ± 1	Sa	0.057	69
5339 NED01	7.4	2.5	0.2 ± 0.2	98 ± 20	26 ± 1	Gpair	0.035	...
12906	12.4	3.1	0.6 ± 0.1	78 ± 4	73 ± 1	S0/a	0.081	55

^aThis galaxy was observed during both observing runs to check for consistency. The average values over both observing runs are quoted here.

^bThe position angle quoted in NED was used instead of the calculated value.

Note. — Listed here for each galaxy are the radius r and σ_G used in the Gaussian weight function G (Equation 1), linear percent polarization, polarization angle, position angle, morphological type, MW extinction $E(B - V)$, and the inclination angle. The morphological types and Milky Way extinction $E(B - V)$ are from NASA's Extragalactic Database (NED) (de Vaucouleurs et al. 1991; Burstein & Heiles 1982). The inclination angles were derived from NED (Equation 9) (Nilson 1973). All data below the line were not used in the data analysis (for details please see text).

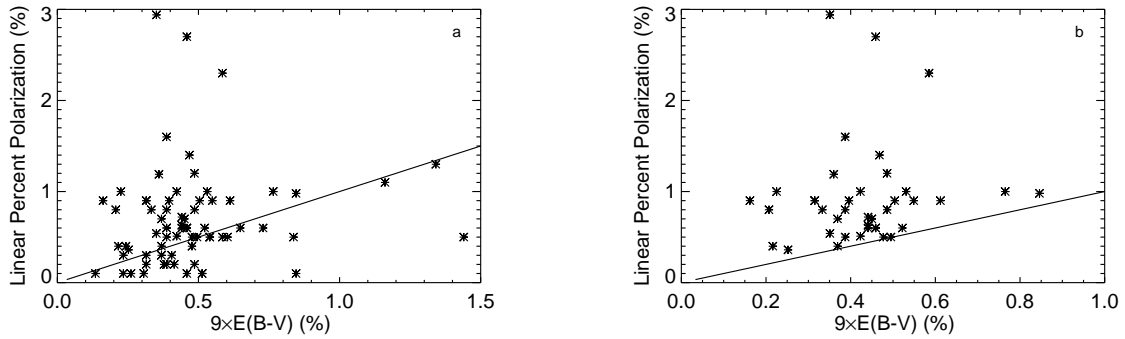


Fig. 1.— The linear polarization (%) versus the maximum MW foreground extinction $\sim 9 \times E(B - V)$ (%). The left plot (a) shows all the observed galaxies and the right plot (b) shows only the accepted detections that were used in the analysis. The galaxies used in the data analysis have levels of linear polarization that are greater than $9 \times E(B - V)$ and are above the 2σ detection limit. See § 2 for more details.

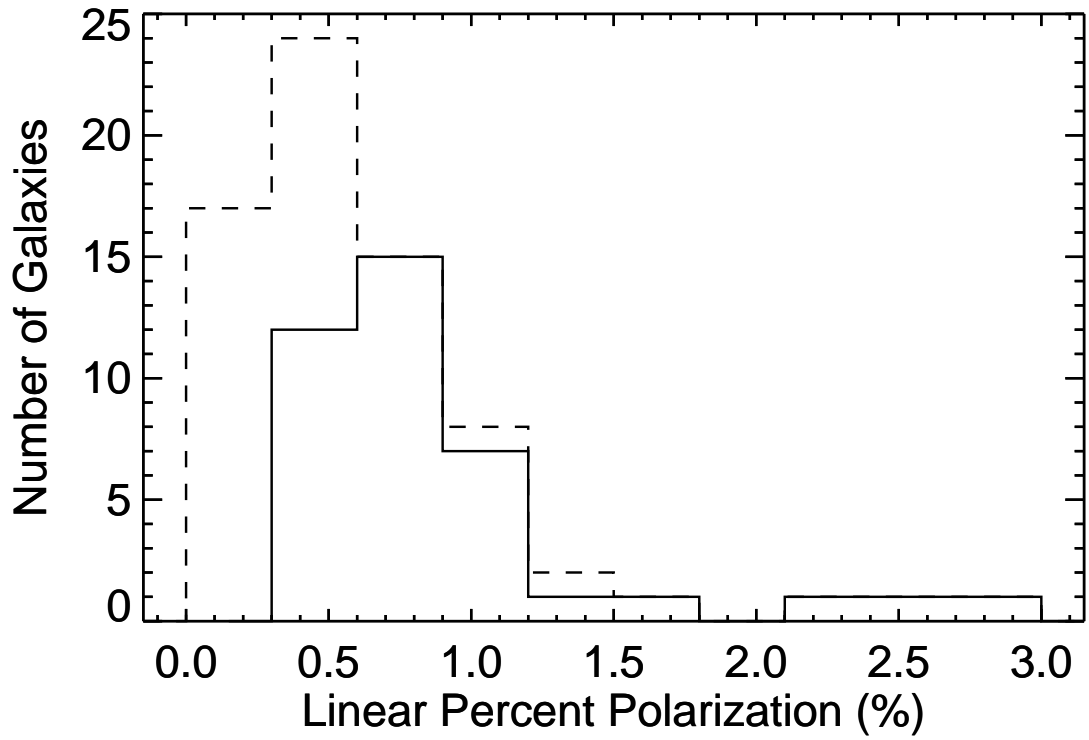


Fig. 2.— A histogram of the distributions of the linear polarization (%), with bin size of 0.3%. All the observed galaxies (dashed line) peak around 0.5%. After the extinction and error cuts (§ 2), the galaxies that are used in the analysis (solid line) have an average polarization of 0.9%.

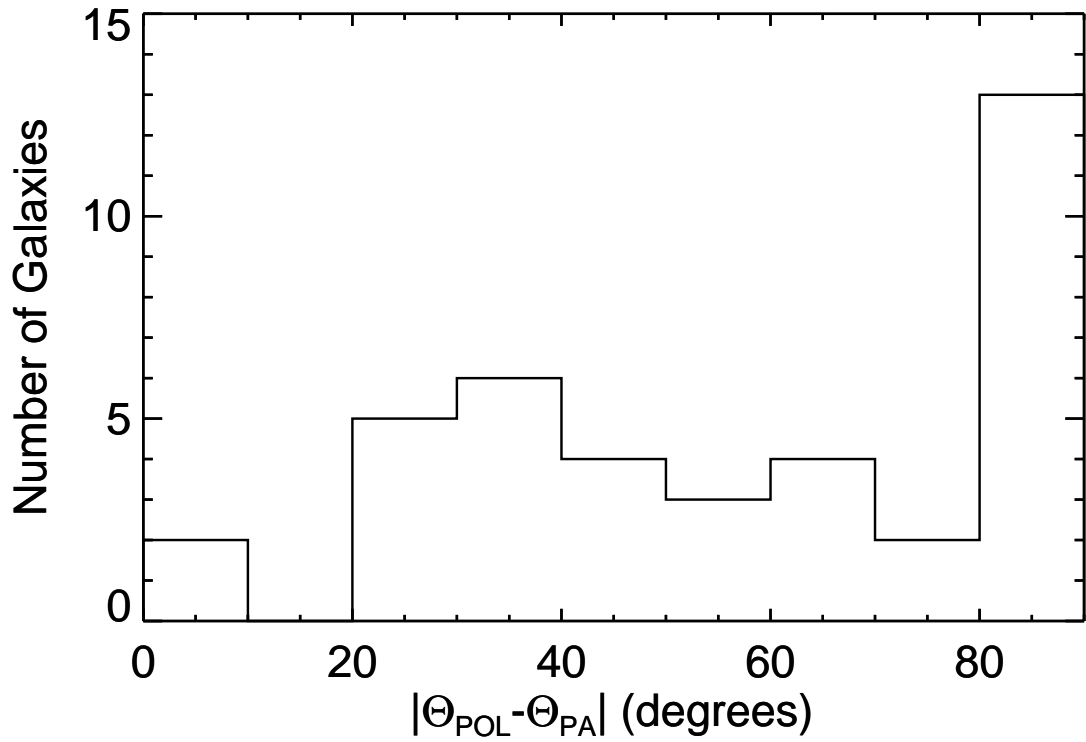


Fig. 3.— A histogram of the distribution of the positive difference between the polarization and position angles, with bin size of 10° . The difference was then folded about 90° . The peak between 80 and 90° means that the polarization angle is perpendicular to the position angle of the galaxy. This suggests that scattering is the dominant source of optical polarization in these galaxies.

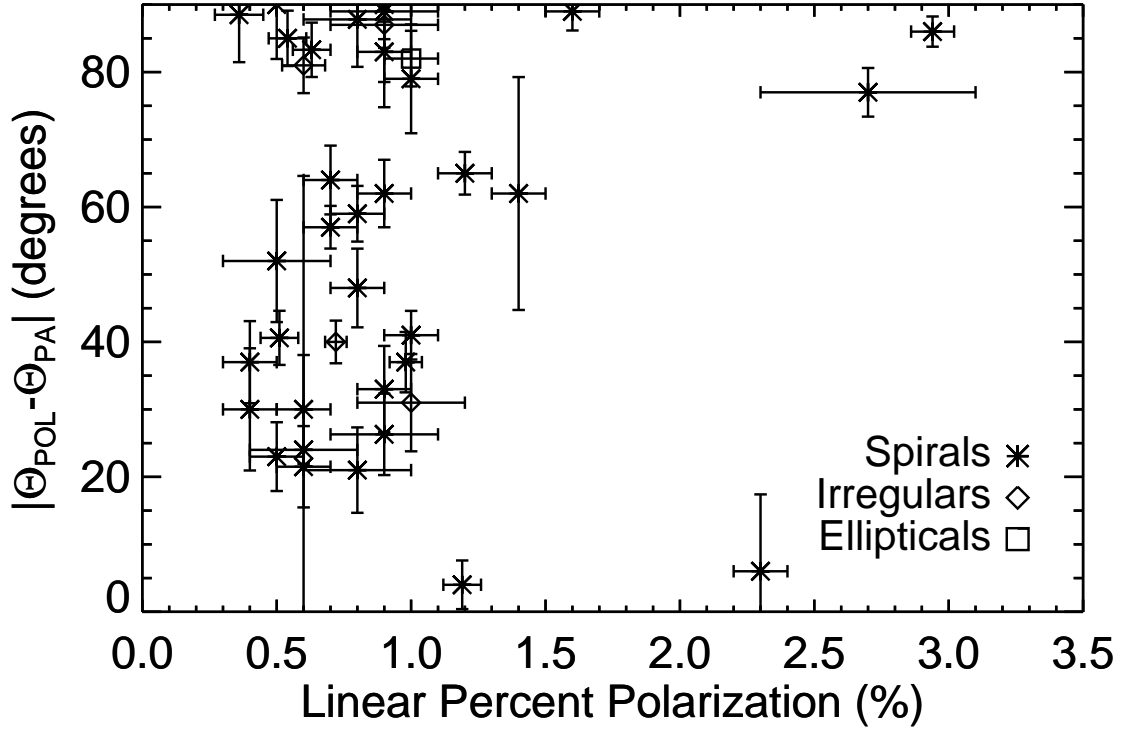


Fig. 4.— A plot of the linear polarization versus the positive difference between the polarization and position angle, with 1σ error bars. Spirals are the stars, irregulars are the diamonds, and the one elliptical is a square. There is a high amount of scatter in the angle below 1% polarization. The highly polarized galaxies, above 1.5%, all have the difference between their polarization and position angles between 77 and 90° , indicating that their polarizations are caused by scattering. The exception is UGC 545, a known Seyfert 1 galaxy, which is parallel (around 0°).

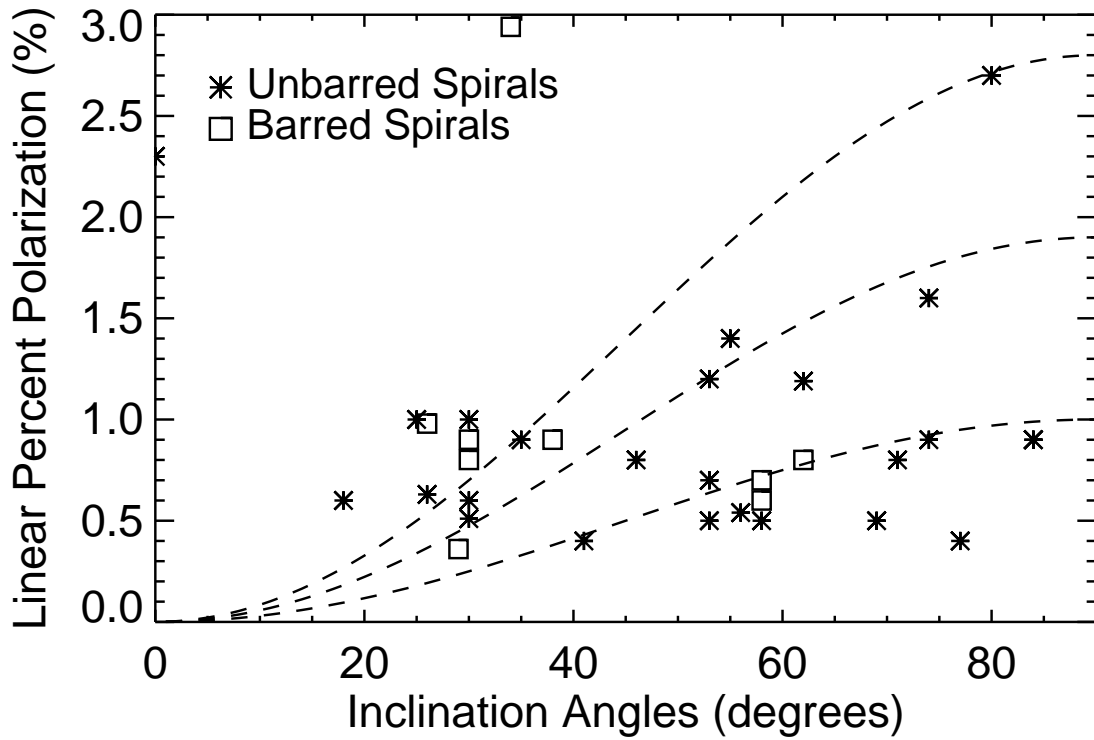


Fig. 5.— A plot of the linear polarization as a function of inclination angle. The squares are the barred spirals and the stars are the unbarred spirals. The barred spirals tend to have a flat distribution compared with the unbarred spirals that peak at high inclinations. Overplotted are the theoretical predictions based on Thomson scattering for $P \sim \sin^2 i$ (Simmons & Audit 2000). The unbarred galaxies roughly follow these predictions. A similar result was seen with radio polarization by Stil et al. (2009).